Study of the consolidation using a pressuremeter apparatus

Jacques Monnet
Gaiatech, Seyssinet, France, monnet.jacques@gaiatech.fr

Luc Boutonnier
EGIS, Seyssins, France, luc.boutonnier@egis-group.com

ABSTRACT: This study demonstrates that the pressuremeter test (PMT), with pore pressure measurement, can measure key parameters for soil consolidation theory. Traditional interpretations assume linear elasto-plastic behavior and do not take into account pore pressure increase. We propose a new approach: by modelling the compressible interstitial fluid (water-air mixture) and accounting for non-linear soil elasticity, PMT can estimate both the effective modulus and generated pore pressure. The consolidation process around the probe is shown to follow a one-dimensional radial pattern, similar to oedometer tests, governed by the consolidation coefficient c_h. Using theoretical developments and experimental validation on Bransley clay, we establish a direct relationship between pore pressure dissipation and time, enabling the determination of c_h and the Skempton coefficient from PMT data. Laboratory and in-situ tests confirm the method's accuracy, even without full pore pressure dissipation. These results position PMT as a practical tool for assessing soil consolidation and effective soil parameters, offering a new way to analyse soil behaviour, in addition to conventional methods.

KEYWORDS: Consolidation, Pore pressure, Pressuremeter.

1 INTRODUCTION

The pressuremeter test (PMT) is not only a tool for measuring soil stiffness but also a means to directly assess soil consolidation parameters. While traditionally interpreted using linear elasto-plastic models, PMT with pore pressure measurements can capture the influence of permeability and saturation on drained or undrained behavior, providing insights into whether the measured modulus is effective or apparent. Recent advances within the ARSCOP project have enabled the calculation of the effective modulus for nearly saturated fine soils, where the pore fluid—a compressible water-air mixture—plays a critical role (Boutonnier, 2007). This approach allows for the estimation of both the effective modulus and the pore pressure generated during testing, as the probe expands and the soil deforms.

By incorporating the non-linear elastic response of the soil skeleton, using a G/Gmax law as a function of strain (Monnet and Boutonnier, 2025), PMT reveals its potential to characterize consolidation. Historically, the generation of pore pressure during PMT has been debated: although theory suggests no volume change under shear, field measurements in clay consistently show pore pressure increases linked to probe expansion (Clarke et al., 1979; Alzubaidi, 2019). We have demonstrated that this phenomenon arises from the soil's non-linear elasticity (Monnet and Boutonnier, 2024), which enables PMT to monitor the dissipation of pore pressure in fine soils. This dissipation follows a one-dimensional radial consolidation process, analogous to vertical consolidation in oedometers—a mechanism often overlooked in previous experimental (Baguelin et al., 1972), analytical (Baguelin, et al., 1978) or pile-focused studies (Niarchos, 2012).

This study formalizes how PMT can measure the consolidation coefficient c_h, which depends on the compressibility of the interstitial fluid and horizontal permeability k_h. By explicitly defining the effective stress state along the radius and validating the approach with Bransley clay data (Anderson et al., 1987), we show that PMT provides a robust method for evaluating consolidation, distinguishing the roles of pore water and the solid skeleton over time.

2 THEORY – HYPOTHESIS

The following hypothesis are used in this study

2.1 *Coordinate*

In the context of the pressuremeter (Figure 1), a total pressure p is applied to the borehole wall at radius a, and the pore pressure u_w is measured at the borehole wall. The analysis is conducted using cylindrical coordinates.

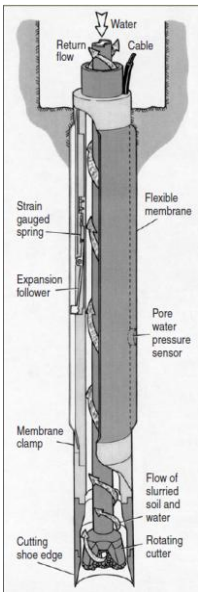

Figure 1: The pressuremeter used (Whittle, 2019)

2.2 *Mass conservation*

We note ε_v the volume variation of the element of soil. $\vec{V}$ is the speed of the interstitial fluid which move only on the radial direction $V_\theta = 0$ et $V_z = 0$. The mass conservation implies:

$$\frac{\partial \varepsilon_v}{\partial t} = -\frac{1}{r}.\frac{\partial (r.V_r)}{\partial r} = -\frac{1}{r}.V_r - \frac{d(V_r)}{dr} \qquad (1)$$

2.3 *Darcy Law*

The Darcy law is applied Equation (2), which gives a relation between the water speed V_r along the radius r and the variation of the pore pressure u_w : with k_h soil permeability; γ_w the bulk

Data sensitivity - Internal

density of the interstitial fluid. This relation introduce into Equation (1) allows finding the relation between the volume variation and the pore pressure from the Darcy equation:

$$V_r = -\frac{k_h}{\gamma_w}.\frac{\partial u_w}{\partial r} \quad (2)$$

$$\frac{\partial \varepsilon_v}{\partial t} = -\frac{k_h}{\gamma_w}.\left(\frac{1}{r}.\frac{\partial u_w}{\partial r} + \frac{\partial^2 u_w}{\partial r^2}\right) \quad (3)$$

2.4 *Relation between volume variation and pore pressure :*

Previous studies have demonstrated that the interstitial fluid consists of water and air bubbles, even in soils typically considered saturated (Monnet and Boutonnier, 2024). For this compressible fluid, volume changes are related to the compressibility coefficient c_f of the water-air mixture, and n the constant porosity of the soil.

$$\frac{d\varepsilon_v}{dt} = -c_f.n.\frac{du_w}{dt} \quad (4)$$

2.5 *Terzaghi condition:*

The total pressure p is applied to the borehole wall at radius a. It is considered constant and independent of time. Consequently, the total pressure σ at any radius is also constant over time. The Terzaghi relation links it to the effective pressure σ‘ and the pore pressure Equation (5). This gives Equation (6):

$$\sigma = \sigma' + u_w = Cte \quad (5)$$

$$\frac{\partial \sigma'}{\partial t} = -\frac{\partial u_w}{\partial t} \quad (6)$$

2.6 *Non-saturation condition:*

It is assumed that the soil is in D3 state (Boutonnier, 2007), i.e saturation with water and air bubbles; this leads to c_h the apparent consolidation coefficient, with c_f the compressibility coefficient of the mix soil + fluid + air; γ_w is the unit weight of the water; n is the porosity of the soil Equation (7).

$$c_h = \frac{k_h}{\gamma_w.c_f.n} \quad (7)$$

2.7 *Small strain*

To simplify the theory, it is assumed small strains

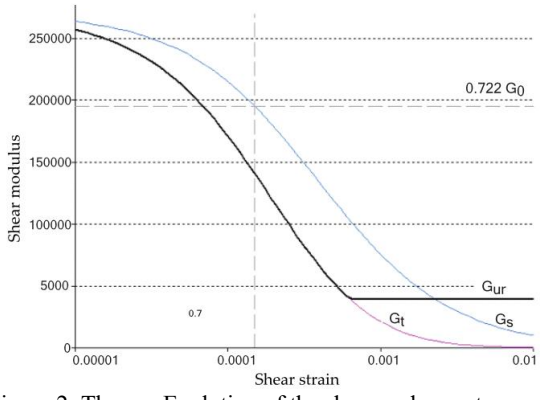

Figure 2: Theory :Evolution of the shear and secant modulus assumed (Plaxis corp., 2015)

2.8 *Non-linear elasticity*

A non-linear elasticity is assumed (Figure 2) so that the apparition of the pore pressure is possible (Monnet and Boutonnier, 2024), where the shear modulus depends on the shear strain.

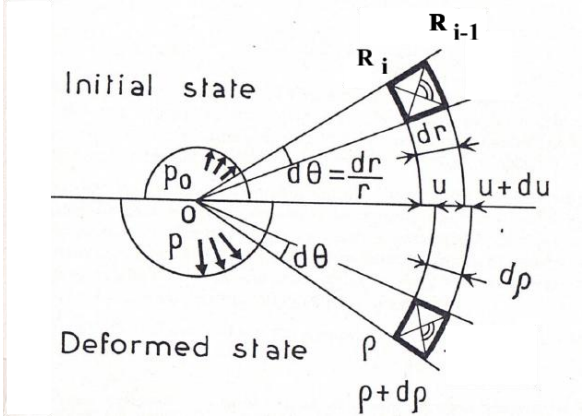

Figure 3: Equilibrium and Strain of the Elementary Prism in the Horizontal Plane (Baguelin, et al., 1978)

3 THEORY – DEVELOPMENTS

3.1 *Relation between pore pressure, strain and total stress*

Considering a circular annulus (Figure 3) between radii Ri and R_{i-1}. This annulus has a cross-section S Equation (8) and deforms under the action of the borehole pressure, with its variation being dS Equation (9). Noting that dR_i is the displacement u_i and dR_{i-1} is the displacement u_{i-1}, the equation allows for the determination of the volume variation by Equation (11). For an elastic behavior the numerator is null, but for an inelastic behavior (Figure 2) the value of $\varepsilon_{\theta i}$ is larger than the linear elastic result, so that the volume decreases and the interstitial pressure increases. We propose Equation (12) for the relation between volume variation and pore pressure. In this demonstration we use the consequences of our previous study (Monnet and Boutonnier, 2025) where elastic strains ε_r and ε_θ are symmetrical and elastic effective stresses σ'_r and σ'_θ are symmetrical from the effective horizontal initial pressure at rest p'_0 .

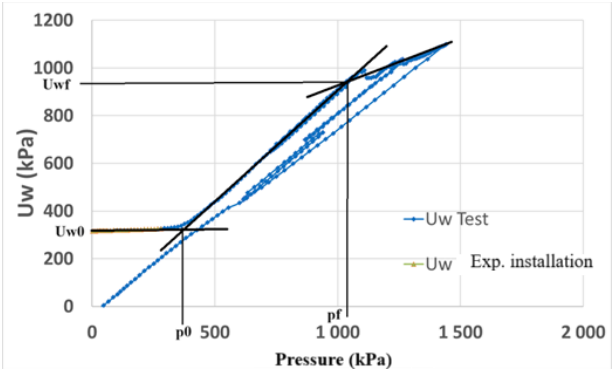

Figure 4: Experience : linear relation between the measured pore pressure and the total pressure – pressuremeter test in London clay at 20,8m depth (Monnet and Boutonnier, 2024)

$$S = \pi.\left(R_{i-1}^2 - R_i^2\right) \quad (8)$$

$$dS = \pi.\left(2.R_{i-1}.dR_{i-1} - 2.R_i\ .dR_i\ \right) \quad (9)$$

$$\varepsilon_v = \frac{dS}{S} = \frac{\left(2.R_{i-1}.u_{i-1} - 2.R_i\ .u_i\ \right)}{\left(R_{i-1}^2 - R_i^2\right)} \quad (10)$$

Data sensitivity - Internal

$$\varepsilon_v = \frac{dS}{S} = \frac{\left(2.R_{i-1}^2.\varepsilon_{\theta i-1} - 2.R_i^2.\varepsilon_{\theta i}\right)}{\left(R_{i-1}^2 - R_i^2\right)} \quad (11)$$

$$\delta u_{wi} = -\frac{\delta\varepsilon_v}{c_f.n} = \frac{2.\delta\varepsilon_{\theta i}}{c_f.n} = \frac{\delta\sigma'_{ri}}{c_f.n.G_s'} \quad (12)$$

From Equation (12) the relationship between Pore Pressure and Total Stress is derived, leading to the expression of the coefficient B_{pres} Equation (15), which is the second Skempton coefficient (Skempton, 1954).

$$\delta\sigma_r = \delta u_{wi} + \delta u_{wi}.c_f.n.G_s' \quad (13)$$

$$\delta\sigma_r = \delta u_{wi}.\left(1 + c_f.n.G_s'\right) \quad (14)$$

$$\frac{\delta u_{wi}}{\delta\sigma_r} = \frac{1}{\left(1 + c_f.n.G_s'\right)} = B_{pres} \quad (15)$$

This relation can be found experimentally (Figure 4) in the elastic part of the behaviour (400kPa < p < 1000kPa).

3.2 *Consolidation equation*

Combining Equations (3) and (4), we find the consolidation Equation (16) which can be rewritten into Equation (18)

$$-c_f.n.\frac{du_w}{dt} = -\frac{k_h}{\gamma_w}.\frac{1}{r}.\frac{\partial(r.u_w)}{\partial r} \quad (16)$$

$$\frac{\gamma_w.c_f.n}{k_h}.\frac{du_w}{dt} = \frac{1}{r}.\frac{\partial(r.u_w)}{\partial r} \quad (17)$$

$$\frac{\gamma_w.c_f.n}{k_h}.\frac{du_w}{dt} = \frac{1}{c_h}\frac{du_w}{dt} = \left(\frac{d^2u_w}{dr^2} + \frac{1}{r}.\frac{du_w}{dr}\right) \quad (18)$$

3.3 *Separation of variables*

To solve Equation (18), we assume that the solution is of the form Equation (19). This gives a new Equation (20), with u_{w0} the constant initial pressure.

$$u_w(r,t) = X(r).T(t) + u_{w0} \quad (19)$$

$$\frac{1}{c_h}.X(r)\frac{dT(t)}{dt} = \left(\frac{d^2X(r)}{dr^2}.T(t) + \frac{1}{r}.\frac{dX(r)}{dr}.T(t)\right) \quad (20)$$

Dividing by $X(r).T(t)$ we find Equation (21). In Equation (21) the left part depends on the time, while the right part depends on the space. This is only possible if each parts of Equation (21) is equal to the same constant $-\lambda^2$.

$$\frac{1}{c_h}.\frac{1}{T(t)}\frac{dT(t)}{dt} = \left(\frac{1}{X(r)}.\frac{d^2X(r)}{dr^2} + \frac{1}{r.X(r)}.\frac{dX(r)}{dr}\right) = -\lambda^2 \quad (21)$$

3.4 *Solution depending on the time*

The time part of Equation (21) is now Equation (22) and can be solved by Equation (23). The condition of T(t)=1 for t=0 gives T_0=1. The constant exponent ω is the slope of the relation between the Logarithm of the increase of pore pressure versus the time. It is an experimental coefficient of the model.

$$\frac{1}{T(t)}.\frac{\partial T(t)}{\partial t} = -\lambda^2.c_h = -\omega \quad (22)$$

$$T(t) = T_0.exp^{-\lambda_n^2.c_h.t} = exp^{-\lambda_n^2.c_h.t} = exp^{-\omega.t} \quad (23)$$

3.5 *Solution depending on the radius*

The spatial part of Equation (21) is now Equation (24) and is transformed multiplying X(r) into Equation (25).

$$\left(\frac{1}{X(r)}\frac{\partial^2 X(r)}{\partial r^2} + \frac{1}{r.X(r)}.\frac{\partial X(r)}{\partial r}\right) = -\lambda^2 \quad (24)$$

$$\frac{\partial^2 X(r)}{\partial r^2} + \frac{1}{r}.\frac{\partial X(r)}{\partial r} + \lambda^2.X(r) = 0 \quad (25)$$

Equation (25) is in the form of a Bessel equation of order zero. It solution is known as Equation (26) with the Bessel functions of first order J_0 and Y_0, and the constants A and B.

$$X(r) = A.J_0(\lambda.r) + B.Y_0(\lambda.r) \quad (26)$$

3.6 *Condition on radius – no pore pressure after $L_d.a$*

At a distance of $L_d.a$ the increase of pore pressure given by the pressuremeter is null. This condition gives the equations (27) (28) with the value of B and J_0 to be null.

$$X(\lambda.L_d.a) = A.J_0(\lambda.L_d.a) + B.Y_0(\lambda.L_d.a) = 0 \quad (27)$$

$$B = -A.\frac{J_0(\lambda.L_d.a)}{Y_0(\lambda.L_d.a)} = \alpha.A \quad (28)$$

$$\alpha = -\frac{J_0(\lambda.L_d.a)}{Y_0(\lambda.L_d.a)} \quad (29)$$

3.7 *Condition on radius -impermeability – determination of λ.*

At the radius a of the pressuremeter there is no flow; the border is impermeable. This implies:

$$\frac{dX(a)}{dr} = A.J'_0(\lambda.a) + B.Y'_0(\lambda.a) = 0 \quad (30)$$

Using relation (28) and the properties of Bessel function equation (30) can be rewritten into (31) which gives after simplification (32):

$$A.J'_0(\lambda.a) - A.\frac{J_0(\lambda.L_d.a)}{Y_0(\lambda.L_d.a)}.Y'_0(\lambda.a) = 0 \quad (31)$$

$$-J_1(\lambda.a).Y_0(\lambda.L_d.a) + J_0(\lambda.L_d.a).Y_1(\lambda.a) = 0 \quad (32)$$

The internal parameter λ is the solution of this equation which can be resolved by numerical methods (Newton-Raphson; bisection; ….)

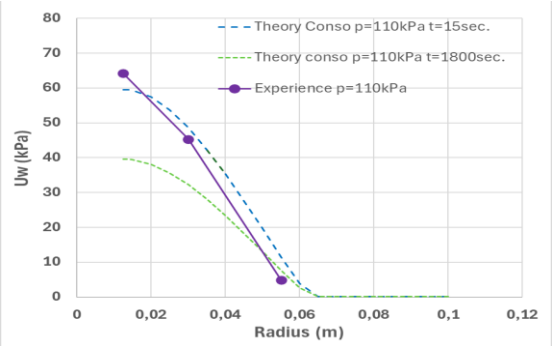

Figure 5: Theory - Evolution of interstitial pressure as a function of radius for different values of consolidation time (total pressure p=110kPa is constant) with the mini-pressuremeter (Anderson, Pyrah and Ali Faisal, 1987a) loading 30kPa/min.

3.8 *Condition on radius – pore pressure at radius a for t=0*

The initial pore pressure at the borehole wall is known. This condition impose $X(\lambda.a) = u_{wi} - u_{w0}$ which give Equation (33) and the value of A Equation (*34*):

$$X(\lambda.a) = A.[J_0(\lambda.a) + \alpha.Y_0(\lambda.a)] = u_{wi} - u_{w0} \quad (33)$$

$$A = (u_{wi} - u_{w0})/J_0(\lambda.a) + \alpha.Y_0(\lambda.a) \quad (34)$$

Please note that the initial pore pressure is known through the Skempton Equation (15) where $\delta\sigma_r = \delta p$ and the known value of B_{pres}.

Data sensitivity - Internal

3.9 *General solution of the pore pressure*

The general solution of consolidation is now Equation (36) using notation Equation (35) and u_{w0} the pore pressure before loading; ω is the slope of the linear relation between the increase of pore pressure and the time.

$$\omega = \lambda^2 . c_h \tag{35}$$

$$u_w(r,t) = A.[J_0(\lambda.r) + \alpha.Y_0(\lambda.r)].exp^{-\omega.t} + u_{w0} \tag{36}$$

3.10 *Degree of consolidation of a single loading*

The evolution of the pore pressure along the radius for different consolidation time is known (Figure 5). Then it is possible to determine the degree of consolidation through equation (37).

$$U(t) = \frac{\int_a^{Ld.a} u_{w1}(r,0).dr - \int_a^{Ld.a} u_{w1}(r,t).dr}{\int_a^{Ld.a} u_{w1}(r,0).dr} \tag{37}$$

The integration of the pore pressure equation (36) along the radius is now equation (42), so that the expression of the degree of consolidation is equation (41):

$$I_{1t} = a.A.\exp^{-\omega t}\{Ld.[J_1(\lambda.L_d.a) + \alpha.Y_1(\lambda.L_d.a)]\} \tag{38}$$

$$I_{2t} = a.A.\exp^{-\omega t}.\{-\lambda.Ld[J_1(\lambda.a) + \alpha.Y_1(\lambda.a)]\} \tag{39}$$

$$I_{3t} = I_{1t} + I_{2t} \tag{40}$$

$$U(t) = 1 - \exp^{-\omega t} \tag{41}$$

3.11 *Degree of consolidation of multiple loading*

For the case of multiple loading, we must realise the integration of equation (51), which is Equation (44), and after reduction the final form of U(t) is now Equation (45). The consolidation of each loading is accounted for independently and is a simplification of the real physic of the phenomenon.

$$I_4 = a.\frac{B_{pres}.\delta p.exp^{-\omega.t}}{J_0(\lambda.a) + \alpha.Y_0(\lambda.a)} \tag{42}$$

$$I_5 = \{L_d[J_1(\lambda.L_d a) + \alpha.Y_1(\lambda L_d a)] - \lambda[J_1(\lambda a) + \alpha.Y_1(\lambda a)]\} \tag{43}$$

$$I_6 = I_4.\sum_{j=1}^{j=i} exp^{\omega.t_{cj}}.I_5 \tag{44}$$

$$U(t) = (\exp^{-\omega.t_{cj}} - \exp^{-\omega.t})/\exp^{-\omega.t_{cj}} \tag{45}$$

3.12 *Determination of the horizontal consolidation coefficient c_h*

The definition of ω is equation (35) where ω is measured (see Figure 8 and Figure 12); it allows determining the horizontal consolidation coefficient c_h :

$$c_h = \omega/\lambda^2 \tag{46}$$

4 EXPERIMENT

4.1 *Validation on laboratory tests (Anderson et al, 1987)*

Anderson performed several test, expanding a 12,5mm radius hole into a sample of clay of 150mm radius (Figure 6). Three pore pressure transductors are set at 12,5mm, 30mm and 50mm. Specimen is Barnsley clay. For the validation of the theory, we used the experimental results where p<110kPa and the Skempton coefficient B_{pres} remains constant and equal to 0.6; for highest values of p, B_{pres} changes, so that we consider that plasticity appears and our theory could not be used. This limitation allows us to be in the range of small deformations hypothesis.

4.1.1 *Loading sequence:*

For this test, a 10kPa increment of pressure is applied in 1min. Then the measurement of the pore pressure is performed 15s. after the load was applied. A consolidation time of 30s. or 120s. is applied after loading as shown (Figure 7). This implies that the next loading is performed after 30s. or 120s. of consolidation.

4.1.2 *Consequence of the loading sequence on the consolidation*

At the borehole wall, relation (36) can be simplified to (47). Considering the loading sequence shown in (Figure 7), where the pressure at the borehole wall is set to p, the increase

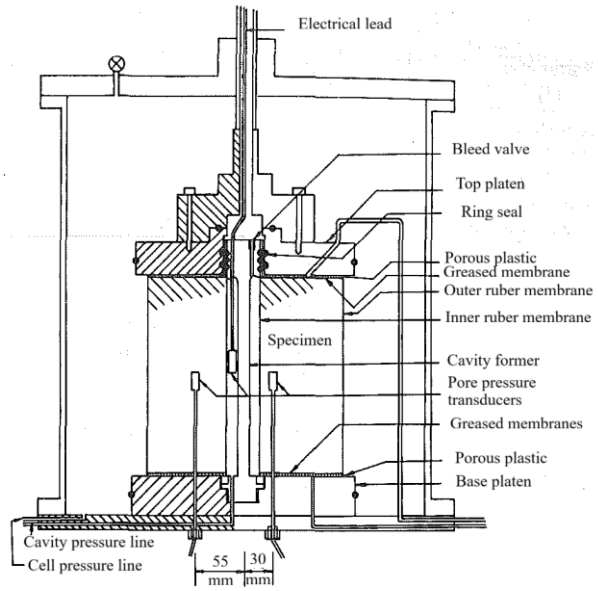

Figure 6: Equipment for hollow cylinder test (Anderson et al., 1987)

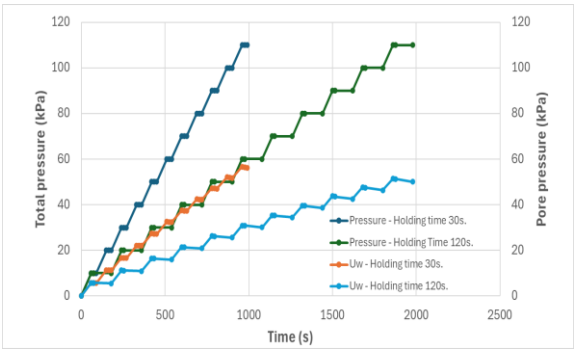

Figure 7: Loading, measurement and consolidation sequence versus time

in initial pore pressure is determined by B_{press}. The time allowed for consolidation is the difference between the total time t and the time at the beginning of consolidation t_{c1}, as described by relation (47). For a new loading phase i, the pore pressure at the borehole can be calculated using equation (48). The equation (48) is independent of the radius and depends only on the total time t and on the beginning time of each consolidation step. It is also possible to get the pore pressure to current radius r (51)

$$u_w(a,t) = B_{pres}.\delta p.exp^{-\omega.(t-t_{c1})} + u_{w0} \tag{47}$$

$$\delta u_{wi}(a,t) = B_{pres}.\delta p\,.exp^{-\omega.t}\sum_{j=1}^{j=i} exp^{\omega.t_{cj}} \tag{48}$$

Data sensitivity - Internal

$$u_{wi}(a,t) = u_{w0} + \delta u_{wi}(a,t) \quad (49)$$

$$I_7 = B_{pres}.\delta p.\frac{[J_0(\lambda.r) + \alpha.Y_0(\lambda.r)]}{J_0(\lambda.a) + \alpha.Y_0(\lambda.a)}.exp^{-\omega.t} \quad (50)$$

$$u_{wi}(r,t) = I_7.\sum_{j=1}^{j=i} exp^{\omega.t_{cj}} + u_{w0} \quad (51)$$

These considerations allows us to use these measurements (Anderson et al., 1987) for a validation of our theory. The parameters used are presented (Table 1).

4.1.3 *Measurement of linear relation ω between the decrease of pore pressure and the time:*

At a given value of the radius, for the Barnsley clay specimen, for instance r = a, the consolidation theory shows an exponential relation between the increase of pore pressure versus the time of slope $-\omega = -\lambda^2.c_h$ Equations (35) (36). This theoretical result is retrieved experimentally by the linear relation between the logarithm of the excess of pore pressure versus the time (Figure 8). The mean value of the slope ω is shown (Table 1).

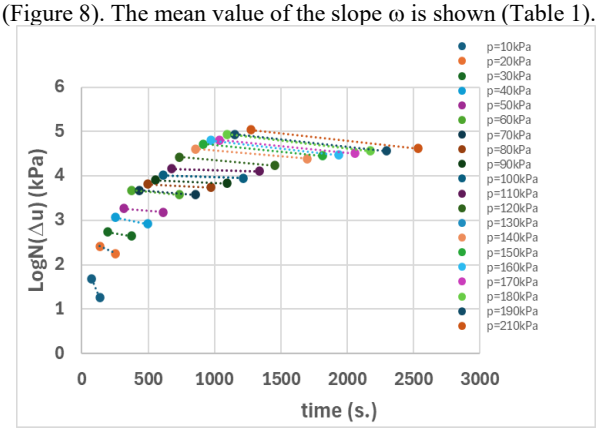

Figure 8: Evolution of the increase of pore pressure along time for different values of loading

Table 1 : Parameters used for the validation of the consolidation theory on the laboratory test (Anderson et al., 1987)

Parameter	Symbol	Value
Pressuremeter Radius	a (m)	$1.25.10^{-2}$
Initial Pore pressure	u_{w0} (kPa)	0
Skempton coefficient	B_{pres}	0.60
Initial pressure at rest	p_0 (kPa)	0
Influence length pressuremeter	L_d	5
Slope Ln (Δu) - t	ω (kPa/s)	$2.3.10^{-4}$

4.1.4 *Evolution of the pore pressure along the radius:*

For the Barnsley clay specimen, the evolution of pore pressure along the radius was measured after 15 s. (Anderson et al., 1987). This measurement (solid line-Figure 9) can be compared with the results from the consolidation theory (dash line-Figure 9) which coincide quite well with the experimental results at each radius. The theory not only captures the main trend of decreasing pore pressure observed in the experiment but also accurately predicts the same downward curvature as seen in the experimental results. The non drainage condition at the radius of the pressuremeter imposes normality of the theoretical line to the borehole wall.

4.1.5 *Evolution of the pore pressure along the time:*

For the Barnsley clay specimen (Anderson et al., 1987), the experimental results are compared to theoretical predictions based on consolidation theory. Both sets of calculations utilize the same parameters, which are detailed in Table 1. In Figure 10 and Figure 11, the experimental data is depicted with solid

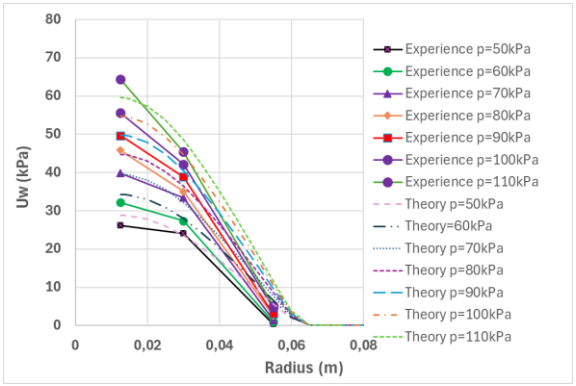

Figure 9: Evolution of the pore pressure along the radius for test with Δp=10kPa/Min, holding time 30s.

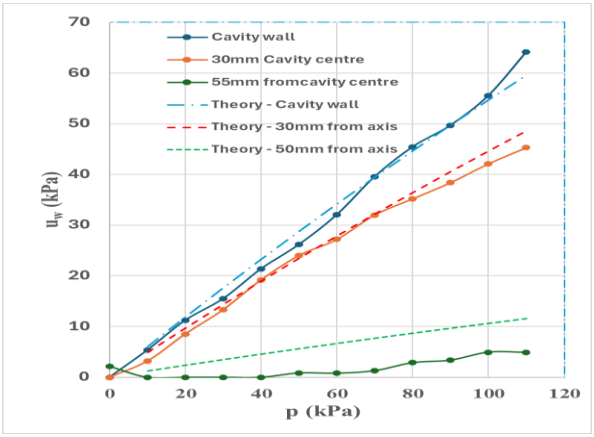

Figure 10: Evolution of the pore pressure along the radius for test with Δp=10kPa 15s. after loading 30s., holding time

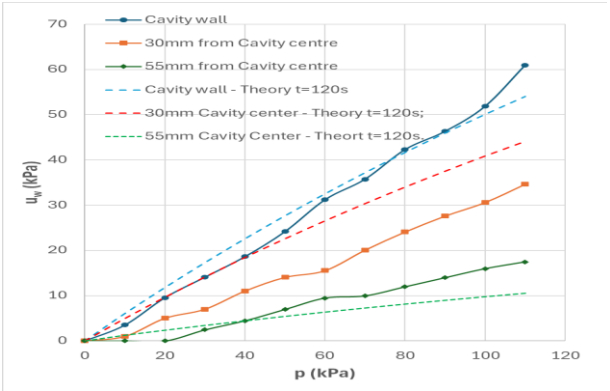

Figure 11: Evolution of the pore pressure along the radius test with Δp=10kPa 15s. after loading, 120s. holding time

lines, while theoretical results are indicated with dotted lines. The pore pressure evolution was recorded at the cavity wall for both experiments. However, in Figure 10, the measurement taken 30 mm from the center is lower than the theoretical prediction, and the measurement at 55 mm is higher. Despite these discrepancies, the overall trends in pore pressure evolution are generally well represented by the theory. The evolution of pore pressure at the borehole wall is consistently captured.

Data sensitivity - Internal

4.1.6 *Measurement of the horizontal consolidation coefficient c_h :*

From a pressuremeter perspective, the slope ω = 0.00023 is determined from the mean slope of regression lines between p=20 and 110kPa (Figure 8). Using equations (32) (35) and (46), we obtain λ = 41,40 and $c_h = 1.34 \times 10^{-7}$ m²/s. The consolidation coefficient c_h is not addressed in (Anderson et al., 1987) and cannot be compared.

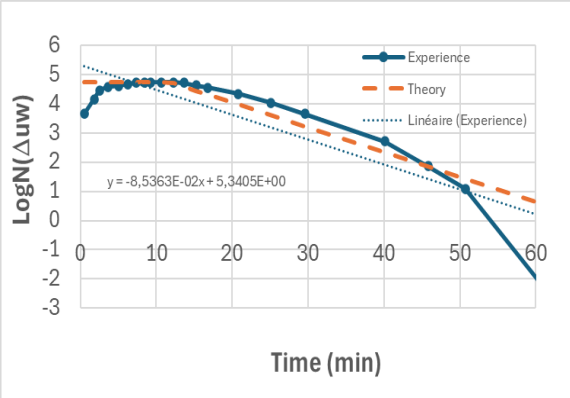

Figure 12: Relation Log(u_w) versus time for the test of (Clarke et al. 1979) - comparison with theoretical results

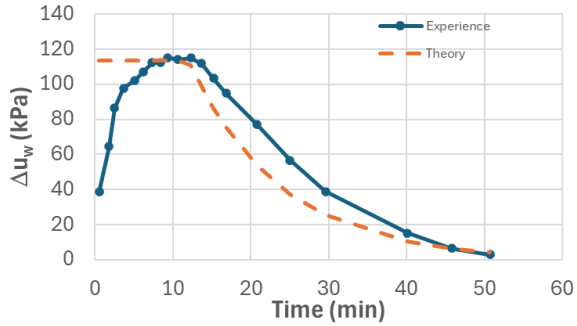

Figure 13: Relation pore pressure versus time for the test of (Clarke et al. 1979) - comparison with theoretical results

4.2 *Validation on in situ tests (Clarke et al. 1979)*

4.2.1 *Measurement of linear relation ω between the decrease of pore pressure and the time:*

Clarke et al. (1979) present the evolution of pore pressure over time (solid line - Figure 12). As predicted by the theory, a linear relationship is observed between the logarithm of the increase of pore pressure (Log(Δu)) versus time, with a theoretical slope -w given by equations (35) (36). This slope is measured to be 0.0085kPa/min, which is equivalent to w=0.000142 kPa/s. The theoretical results (dotted line - Figure 12) find a line with the same slope.

4.2.2 *Prediction of pore pressure along the time:*

The use of equation (36) allow us to retrieve the experimental results (Figure 13) and the evolution of the pore pressure along the time, with the same curvature than the experiment. The parameters used for this calculation are shown (Table 2).

4.2.3 *Measurement of the horizontal consolidation coefficient c_h :*

Applying equations (35) and (46) with the slope ω (Column 3, Line 7, Table 2) allows us to determine λ = 57.03 and $c_h = 4.36 \times 10^{-7}$ m²/s for a pressuremeter with a radius of 35.2 mm. The consolidation value obtained by Clarke et al. (1979) from the U_{50} consideration is very close: $c_h = 4.4 \times 10^{-7}$

Table 2 : Parameters used for the validation of the consolidation theory on in situ test (Clarke et al. 1979)

Parameter	Symbol	Value
Pressuremeter Radius	a (m)	$3.52.10^{-2}$
Initial Pore pressure	u_{w0} (kPa)	0
Skempton coefficient	B_{pres}	0.68
Initial pressure at rest	p_0 (kPa)	0
Influence length pressuremeter	L_d	5
Slope Ln (Δu)-t	ω (kPa/s)	$1.42.10^{-3}$

m²/s. It should be noted that the pressure p is not completely constant and varies between 160 and 130 kPa, which may explain the slight difference between these two results. Furthermore, linearity is achieved after 40 minutes of consolidation, making subsequent measurements unnecessary.

5 CONCLUSION

This study establishes the pressuremeter test (PMT) with pore pressure measurements as a practical, field-friendly tool for assessing soil consolidation parameters, offering a reliable alternative to traditional oedometer tests, particularly when intact soil sampling is difficult. By linking pore pressure dissipation to time and radius, we provide a direct method to determine the horizontal consolidation coefficient (c_h) and Skempton's coefficient (B_{pres}) without requiring full pore pressure dissipation—only the linear phase needs to be observed. This reduces testing time and cost, making it ideal for real-world geotechnical investigations. The proposed approach enhances the design of foundations, embankments, and earthworks by delivering an additional way to assess soil hydromechanical behaviour, even in partially saturated conditions, with in-situ measurements. However, the method must be improved to be theoretically more relevant for multiple loading consolidation. Future work should focus also on validating the method across diverse soil types and saturation states, as well as integrating it into standardized testing protocols Expanding its application to cyclic or dynamic loading scenarios could further broaden its utility.

6 REFERENCES

Anderson, W.F., Pyrah, I.C. and Ali Faisal, H., 1987. Rate effects in Pressuremeter tests in clays. *Journal of Geotechnical Engineering, ASCE*, 113(11), pp.1344–1358.

Baguelin, F., Jezequel, J.F., Le Mee, E. and Le Mehauté, A., 1972. Expansion de sondes cylindriques dans les sols cohérents. *Bull. Liaison Labo. P. et C h*, (31).

Baguelin, F., Jezequel, J.F. and Shields, D.H., 1978. *The pressuremeter and foundation engineering,*. Switzerland, Trans Tech Pub.

Boutonnier, L., 2007. *Comportement hydromécanique des sols fins proches de la saturation. Cas des ouvrages en terre : coefficient B, déformations instantanées et différées.*Thèse INPG Grenoble.

Clarke, B.G., Carter, J. and Wroth, C.P., 1979. In situ determination of the consolidation characteristics of saturated clays. In: *7th Eur. conf. soil mech. found. eng.,* Brighton. pp.207–211.

Monnet, J. and Boutonnier, L., 2024. Interpretation of the pressuremeter test into clay in unsaturated and undrained condition, *7th Int. Conf. Geot. Geoph.. Site Char*. Barcelonne.

Niarchos, D.G., 2012. *Analysis of consolidation around driven piles in overconsolidated clay*. PhD Thesis. Mass. Inst. Tech..

Plaxis corp., 2015. *Plaxis Version 8 - Material Models Manual*., https://communities.bentley.com

Skempton, A.W., 1954. The Pore-Pressure Coefficients A and B | *Géotechnique*, 4, pp.143–147.

Whittle, R., 2019. Cambridge In Situ - Using pressuremeter. *Cambridge In Situ*. , http://www.cambridge-insitu.com.

Data sensitivity - Internal